

High Dielectric Constant in the Charge-ordered Manganese Oxide $\text{CaMn}_7\text{O}_{12}$

S. Yáñez Vilar^a, A. Castro-Couceiro^a, B. Rivas-Murias^b, A. Fondado^b, J. Mira^b, J. Rivas^b, M. A. Señarís-Rodríguez^{a,*}

^a A Coruña/Spain, Química Fundamental, Universidad de A Coruña

^b Santiago de Compostela/Spain, Física Aplicada, Universidad de Santiago

Received December 2nd, 2004; accepted February 15th, 2005.

Abstract. The dielectric properties of mixed-oxide $\text{CaMn}_7\text{O}_{12}$ are reported. This compound exhibits a high dielectric constant at room temperature ($\epsilon'_r > 10^4$), for frequencies up to 10^4 Hz, values that make it very attractive for potential applications provided that its rather high losses can be minimized.

Complex plane analysis of the obtained data reveal an important extrinsic contribution to these high ϵ'_r values; and also that the

intrinsic dielectric constant of this material is $\epsilon'_{r,\infty} \sim 30$, a value rather high for this type of compounds, that could be related to the electronic process of charge-ordering present in this oxide below 440 K.

Keywords: Dielectric properties; Mixed-oxides; Charge ordering

1 Introduction

Dielectric materials with high dielectric permittivities and low loss factors over a wide frequency range are always of great interest due to the important applications of such properties in many electronic devices, like high-performance capacitors. Nowadays, the best industrial performances are given by ferroelectrics, i.e., substances with permanent electrical dipoles, even in the absence of an external electric field [1].

Besides the “classical” and well-known ferroelectric perovskite materials (BaTiO_3 , PbTiO_3 , etc.), that are the most widely used [1], other $\text{ACu}_3\text{M}_4\text{O}_{12}$ (A: Ca, etc.; M: Ti, Fe, etc.) double-perovskites have been recently found [2]. Very interestingly, these latter display very high (giant) dielectric constants, ($\epsilon_r \sim 10^4$ at 300 K) whose intrinsic or extrinsic nature, as well as its origin is being currently intensively debated [2, 3].

In this work we focus in the dielectric properties of $\text{CaMn}_7\text{O}_{12}$, a closely related mixed-oxide that shows the added complexity of experiencing the electronic process of charge ordering as a function of temperature.

From the structural point of view the compound $\text{CaMn}_7\text{O}_{12}$ belongs to the $(\text{AA}'_3)\text{B}_4\text{O}_{12}$ family, as it can be more readily seen when formally writing its formula as: $(\text{CaMn}_3^{3+})(\text{Mn}_3^{3+}\text{Mn}^{4+})\text{O}_{12}$. This perovskite-derived phase, consists of a three-dimensional array of corner-sharing $[\text{BO}_6]$ octahedra, that are tilted, so that one-fourth of the A-sites are distorted into icosahedra (that are occupied by

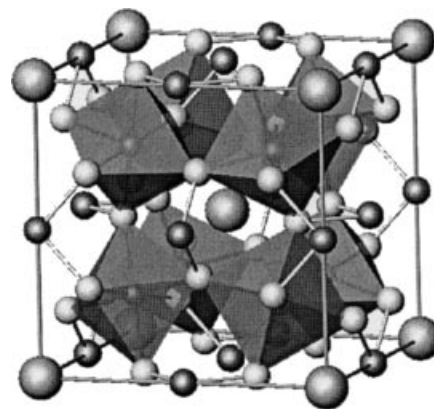


Figure 1 Cubic structure of $\text{CaMn}_7\text{O}_{12}$ ($T > 440$ K).

Ca^{2+} ions) and three-fourths into tetracapped rhombic prisms that accommodate the Jahn-Teller Mn^{3+} ions.

Above 440 K, the formally Mn^{3+} and Mn^{4+} ions occupy at random the octahedral B-sites and the crystal symmetry is cubic ($\text{Im}\bar{3}$) [4] (Figure 1). Nevertheless, at 440 K this compound experiences a structural phase transition associated to the electronic processes of charge and orbital ordering (CO) and (OO) [4]. Below 409 K, the crystal structure has trigonal symmetry (Space group: $\text{R}\bar{3}$) [5], due to the ordering of the distinguishable Mn^{3+} and Mn^{4+} ions in the B sublattice, (9d) and (3b) sites [5]. These two phases coexist over the temperature interval $409 < T < 440$ K.

From the magnetic point of view, this compound is paramagnetic above 86 K. Below 86 K long-range magnetic ordering of the magnetic moments of Mn^{3+} and Mn^{4+} ions has been observed, and between 86 and 50 K two different ordered magnetic phases have been detected: one ferrimagnetic and another modulated [6].

In this paper we study the dielectric behavior of this charge-ordered mixed oxide.

* Prof. Dr. M^a A. Señarís-Rodríguez
Departamento Química Fundamental
Facultad de Ciencias
Universidad de A Coruña
E-15071 A Coruña/Spain
Tel: 34 981 167000
Fax: 34 981 167065
e-mail: tonasr@udc.es

2 Experimental

$\text{CaMn}_7\text{O}_{12}$ was synthesized by the so-called “liquid-mix” or Pechini method [7], using CaCO_3 (Panreac, >98,6 %) and $\text{Mn}(\text{NO}_3)_2 \cdot \text{H}_2\text{O}$ (Aldrich, >98 %) as starting materials. The procedure was as follows: We dissolved stoichiometric amounts of these metallic salts in a 1M citric acid aqueous solution. We then added the same volume of ethyleneglycol, and we finally diluted the so-obtained solution in water (50 % v/v). The resulting solution was heated at 200 °C until a brown resin formed, whose organic matter subsequently decomposed at 400 °C. The precursor powder was treated at 800 °C/48 h, 925 °C/48 h and 950 °C/48 h, with intermediate grindings. Finally it was annealed at the highest temperature of 975 °C (as for $T > 975$ °C the as-obtained sample melts) during 48 h.

The structural characterization of the sample was carried out at room temperature by means of X-ray powder diffraction (XRPD) using a Siemens D-5000 diffractometer and $\text{Cu}(\text{K}\alpha) = 1.5418$ Å radiation. The XRD data were analyzed by the Rietveld profile analysis using the Rietica software [8].

The morphology and particle size of this polycrystalline material was studied in a scanning electron microscope (SEM), JEOL 6400.

The complex dielectric permittivity of this material was measured with a parallel-plate capacitor coupled to a precision LCR meter Agilent 4284 A, capable to measure in frequencies ranging from 20 to 10^6 Hz. The capacitor was mounted in an aluminium box refrigerated with liquid nitrogen, incorporating a mechanism to control the temperature up to 350 K. The pelletized sample with average diameter of 2 cm was prepared to fit in the capacitor, and gold was sputtered on its surface to ensure good electrical contact with the plates of the capacitor. And aware of the controversy regarding extrinsic polarization effects as origin of very high dielectric constants in other ceramic materials [9, 10], additional measurements were performed using sputtered silver contacts.

Also, to test the optimal performance of the experimental set-up, a commercial SrTiO_3 sample was measured and values similar to those reported in the literature [11] were obtained.

Complex plane analysis of the obtained impedance data was performed using the computer program LEVM [12].

3 Results

3.1 Characterization

The X-ray diffraction pattern shows that $\text{CaMn}_7\text{O}_{12}$ is the major phase in the sample but also that small amounts of Mn_2O_3 and Mn_3O_4 are present as secondary phases. Nevertheless, quantitative analysis of the XRD data by the Rietveld method indicate that these impurities represent minor amounts (< 2 %).

This difficulty to obtain a completely pure phase has also been observed and highlighted by other authors, that prepared this mixed oxide by other methods and could neither obtain a single phase material [13].

As for the cell parameters of the $\text{CaMn}_7\text{O}_{12}$ phase, the refinements give $a_h = 10.458$ Å and $c_h = 6.342$ Å in good agreement with the data reported in the literature [13].

Morphologically this polycrystalline sample consists of an homogeneous distribution of pseudo-spherical particles of diameter ≈ 1 μm as seen in the SEM micrographs.

3.2 Dielectric properties

The relative complex dielectric permittivity of the sample: $\epsilon_r = \epsilon'_r - i\epsilon''_r$ ($\epsilon_r = \epsilon/\epsilon_0$; where $\epsilon_0 = 8.85 \times 10^{-12}$ F/m is the permittivity of free space) as well as its conductivity were measured as a function of frequency and temperature.

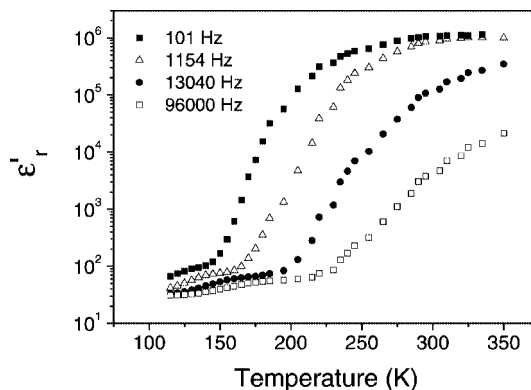


Figure 2 Temperature dependence of the real part of the dielectric permittivity (ϵ'_r) measured at four different frequencies ($101 \leq \nu(\text{Hz}) \leq 96000$).

Figure 2 shows the real part of the dielectric permittivity ϵ'_r (dielectric constant) as a function of temperature, obtained at different frequencies.

The first remarkable feature is that the value of ϵ'_r , that is of the order of 30–50 at low temperatures, experiences a significant increase above a certain temperature giving rise to a very high (giant) dielectric constant at room temperature ($\epsilon'_r > 10^4$). The temperature at which this increase takes place markedly shifts to higher values as the measuring frequency increases.

The behavior of the real part of the dielectric permittivity as a function of frequency is shown in Figure 3. As it can be seen, the giant dielectric constant keeps a constant value for a certain frequency range giving rise to a “plateau”, to then decrease as frequency gets higher. It is also interesting that this plateau extends over larger frequency ranges as temperature gets higher, so that for $T = 300$ K this very high ϵ'_r values ($\epsilon'_r \sim 10^6$) are retained up to 10^4 Hz.

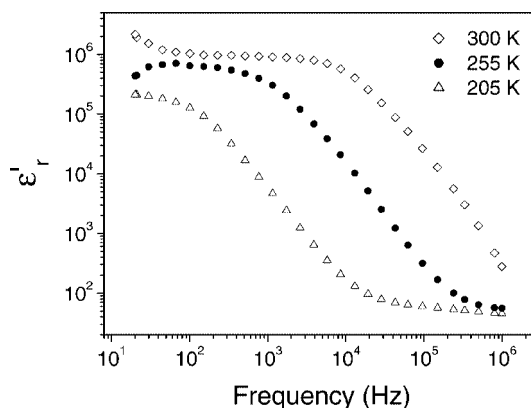


Figure 3 Frequency dependence of the dielectric constant measured at three different temperatures ($205 \leq T \leq 300$ K).

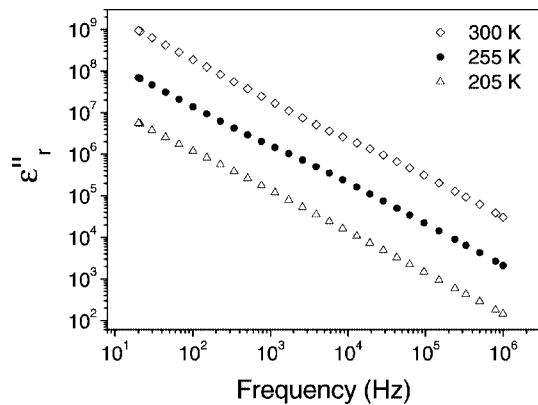


Figure 4 Frequency dependence of the imaginary part of the dielectric constant measured at three different temperatures ($205 \leq T \leq 300$ K).

Meanwhile, the imaginary part of the dielectric permittivity ϵ''_r shows rather high values, that decrease linearly with frequency and increase as temperature rises as shown in Figure 4. As a result, the values of the loss tangent ($\tan \delta$) of this sample, $\tan \delta = \epsilon''_r / \epsilon'_r$, are rather high (Figure 5).

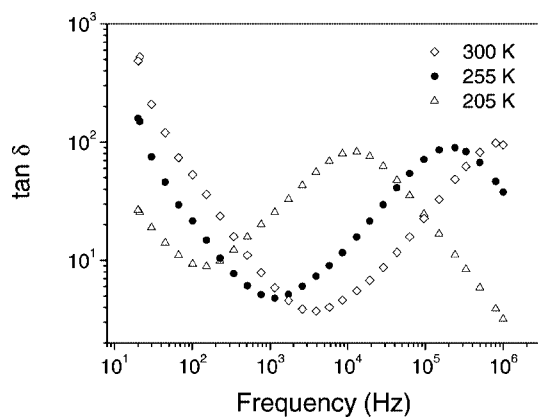


Figure 5 Frequency dependence of loss tangent measured at three different temperatures ($205 \leq T \leq 300$ K).

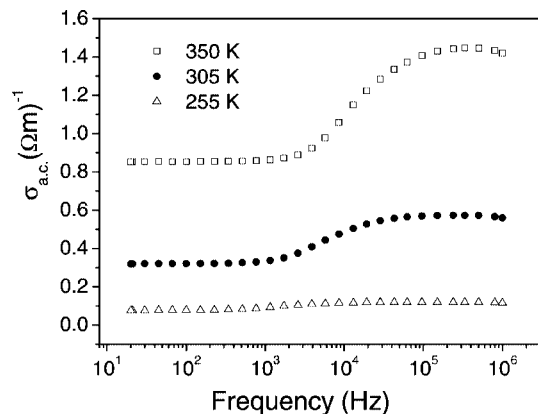


Figure 6 a. c. conductivity versus frequency in the temperature range $255 \leq T \leq 350$ K.

On the other hand, and very importantly, this $\text{CaMn}_7\text{O}_{12}$ sample is not completely insulating but shows a certain conductivity that increases with temperature (Figure 6). In addition, for $T \geq 300$ K the low-frequency $\sigma_{\text{a.c.}}$ constant value experiences a sudden increase at $\nu \approx 10^4$ Hz, that is in fact the frequency at which the dielectric constant shows the step-like decrease.

The here reported results correspond to data obtained using sputtered gold contacts.

If sputtered silver contacts are used slightly smaller ϵ'_r values are measured together with higher loss tangent values.

4 Discussion

The here reported dielectric behavior of the mixed oxide $\text{CaMn}_7\text{O}_{12}$ is very interesting both from the scientific and the technological point of view. In this context, the high dielectric constant of this compound at room temperature for frequencies up to 10^4 Hz makes this material attractive for potential applications provided that its high dielectric losses can be minimized while keeping ϵ'_r as high as possible.

On the other hand, from the scientific point of view many questions should be understood about the origin of the observed dielectric behavior.

For this purpose, and taking into account that this material is not completely insulating, we have subtracted from the ϵ''_r raw data the contribution from free charge carriers following equation [1]:

$$\epsilon''_{\text{r,die}}(\omega) = \epsilon''_r(\omega) - \frac{\sigma_{\text{d.c.}}}{\epsilon_0 \omega} \quad [1]$$

where $\epsilon''_{\text{r,die}}$ is the contribution of the dielectric to ϵ''_r and $\sigma_{\text{d.c.}}$ is the d.c. electrical conductivity, that is obtained from the extrapolation of the conductivity, $\sigma(\omega)$, to low frequencies.

If we represent the so-obtained $\epsilon''_{\text{r,die}}$ data as a function of frequency we find the results shown in Figure 7. As it

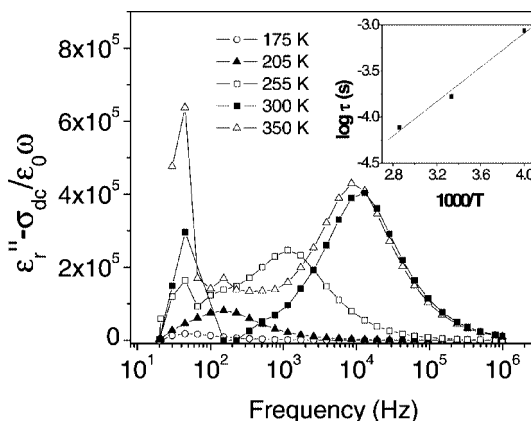


Figure 7 Frequency dependence of the imaginary part of the complex relative dielectric permittivity after subtraction of the contribution from free charge carriers (Temperature range: $175 \leq T \leq 350$ K). Inset: Logarithm of the characteristic time (inverse of the characteristic frequencies) versus the inverse of temperature.

can be seen, in addition to the maximum found at very low frequency –that is typical of diffusional processes– for $T > 250$ K a second maximum appears at $\sim 10^4$ Hz, frequency at which the very high dielectric constant decreases in a step-like manner (Fig. 3). This second maximum resembles that of a Debye-like dipolar relaxation process with characteristic times, $\tau = 1/\omega$, where ω is the characteristic frequency of relaxation.

A logarithmic fit of the characteristic relaxation times versus the inverse of temperature shows that these follow an Arrhenius type of behavior, $\tau = \tau_0 \exp(U/k_B T)$, where U is the activation energy and k_B the Boltzmann constant. From this fit we have obtained a $U \sim 185$ meV and a $\tau_0 \sim 153$ ns.

On the other hand, if we examine the temperature dependence of $\sigma_{\text{d.c.}}$ we observe a thermally activated behavior, with an activation energy of 216 meV.

This result correlates well with that of characteristics times establishing a link between its dielectric relaxation and its conductivity.

But these relaxation process, do they merely come from extrinsic effects due to interfacial polarization (from the electrode/sample interface, from grain boundaries in the polycrystalline sample) as described for other oxides in the literature [14, 15] or do they also have an intrinsic origin in the bulk material?

In this context, the fact that the results are dependent on the contact material already indicate a certain extrinsic contribution [16].

To try to separate extrinsic and intrinsic contributions we have carried out complex plane analysis of the obtained impedance data, which involve plotting the imaginary part (Z'') against the real part (Z') (Figure 8). The data have been best modelled on the basis of an equivalent circuit consisting of two parallel RC elements connected in series, that would represent the contribution from extrinsic factors (grain boundary and/or electrode response), while the bulk response has been approximated by another leaky capacitor, with a bulk capacitance determined by the intrinsic dielectric constant $\epsilon'_{r,1} \approx \epsilon'_{r,\infty}$ and a bulk resistance that is frequency dependent.

This $\epsilon'_{r,\infty}$ is of the order of 30, a value that is still rather high for this type of oxides [17]. In this context it is interesting to note that in our research group we have also detected high dielectric constants in other oxides with charge ordering near their charge ordering temperature, such as in $\text{Pr}_{0.67}\text{Ca}_{0.33}\text{MnO}_3$ [18] ($T_{\text{CO}} \approx 225$ K) were a four fold increase of its dielectric constant is observed as temperature decreases below 225 K. All these results lead us to associate this enhanced intrinsic dielectric constants to the fact that the charge separation that occurs in a CO transition could lead to the formation of some kind of electrical dipoles in these type of materials, as it has also been theoretically proposed by other authors very recently [19].

More work is being done on samples of different particle size, with different geometries and thickness to better clarify the role of extrinsic contributions to the observed dielectric

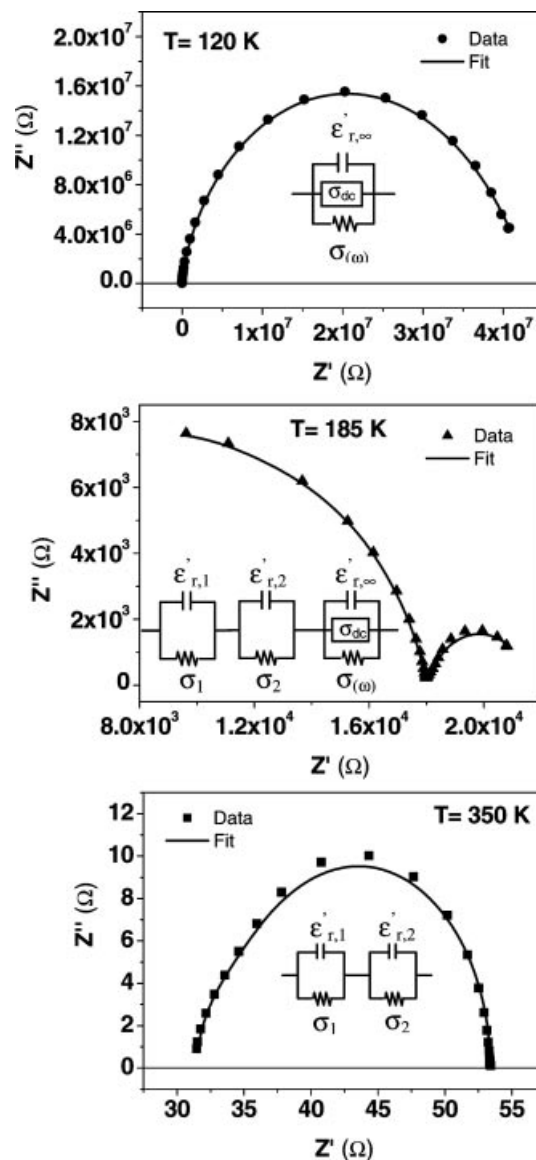


Figure 8 Impedance complex plane plot in three different temperature ranges: for $110 < T < 150$ K the Z^* plot contains a single arc with zero intercept at high frequencies. For $150 < T < 250$ K two arcs appear in the Z^* plot, while for $250 < T < 350$ K a single arc is again seen, but with a non zero intercept in this case. The experimental data have been fitted on the basis of an equivalent circuit consisting of three parallel RC elements connected in series.

response and to optimize the dielectric properties of this interesting material.

Acknowledgments. We thank financial support of the DGI of the Ministry of Science and Technology of Spain under project FEDER MAT 2001-3749.

References

- [1] G. H. Haertling, *J. Am. Ceram. Soc.* **1999**, *82*, 797.
- [2] M. A. Subramanian, L. Dong, N. Duan, B. A. Reisner, A. W. Sleight, *J. Solid State Chem.* **2000**, *151*, 323.
- [3] P. Lunkenheimer, R. Fichtl, S. G. Ebbinhaus, A. Loidl, *Phys. Rev. B* **2004**, *70*, 172102.

- [4] I. O. Troyanchuk, A. N. Chobot, *Crystallogr. Rep.* **1997**, *42*, 983.
- [5] B. Bochu, J. L. Buevoz, J. Chenavas, A. Collomb, J. C. Joubert, M. Marezio, *Solid State Commun.* **1980**, *36*, 133.
- [6] R. Przenioslo, I. Sosnowska, D. Hohlwein, T. Hauß, I. O. Troyanchuk, *Solid State Commun.* **1999**, *111*, 687.
- [7] F. Licci, T. Besagni, L. Rinaldi, **1985** European Patent Appl. No. 85860253-2.
- [8] C. J. Howard, H. Hunter, B. A. Rietica, *A Computer Program for Rietveld Analysis* of Organization Lucas Heights Research Laboratories.
- [9] P. Lunkenheimer, T. Rudolf, A. Hemberger, S. Pimenov, S. Tachos, F. Lichtenberg, A. Loidl, *Phys. Rev.* **2003**, *68*, 245108.
- [10] H. Lixin, J. B. Neaton, M. H. Cohen, D. Vanderbilt, C. C. Homes, *Phys. Rev. B*, **2002**, *65*, 214112.
- [11] R. Viana, P. Lunkenheimer, J. Hemberger, R. Böhmer, A. Loidl, *Phys. Rev. B* **1994**, *50*, 601.
- [12] J. Ross Macdonald, LEVM version 8.0 Complex Nonlinear Squares Fitting Program, 2003.
- [13] R. Przenioslo, I. Sosnowska, E. Suard, A. Hewat, A. N. Fitch, *J. Phys. Condens. Matter* **2002**, *14*, 5747.
- [14] C. J. Maxwell, *Electricity and Magnetism*, Ed. Clarendon Press, Oxford, 1982.
- [15] A. Von Hippel, *Dielectric and Waves*, Ed. Artech House, Boston, London, 1995.
- [16] D. C. Sinclair, T. B. Adams, F. D. Morrison, A. R. West, *Appl. Phys. Lett.* **2002**, *80*(12), 2153.
- [17] P. Lunkenheimer, V. Bobnar, A. V. Pronin, A. I. Ritus, A. A. Volkov, A. Loidl, *Phys. Rev. B* **2002**, *66*, 05215.
- [18] F. Rivadulla, M. A. López Quintela, L. E. Hueso, C. Jardón, A. Fondado, J. Rivas, M. T. Causa, R. D. Sánchez, *Solid State Commun.* **1999**, *110*, 179.
- [19] D. V. Efremov, J. Brink, D. I. Khomskii, *Nature Mater.* **2004**, *3*, 853.